Model Accounting for the Effects of Pulling-Device Stiffness in the Analyses of Single-Molecule Force Measurements

Arijit Maitra and Gaurav Arya*

Department of Nanoengineering, University of California, San Diego, 9500 Gilman Drive, La Jolla, California 92093-0448, USA

(Received 13 September 2009; published 12 March 2010)

Single-molecule force spectroscopy provides a powerful approach for investigating molecular transitions along specific reaction coordinates. Here, we present a general analytical model for extracting the intrinsic rates and activation free energies from force measurements on single molecules that is applicable to a broad range of pulling speeds and device stiffnesses. This model relaxes existing limitations to perform force measurements with soft pulling devices for proper theoretical analyses and, in fact, allows experiments to specifically exploit device stiffness as a control parameter in addition to pulling speed for a reliable estimation of energetic and kinetic parameters.

DOI: 10.1103/PhysRevLett.104.108301 PACS numbers: 82.37.Np, 87.15.ad

Single-molecule force spectroscopy has revolutionized the way thermodynamics and mechanisms of biomolecular processes are studied [1]. These sophisticated techniques involve imposition of controlled forces to single molecules or complexes and relating the observed responses to the characteristics of the underlying molecular free energy landscape. Often, in these experiments, one end of the molecule is held fixed and the other is pulled at a constant speed along the desired reaction coordinate. The applied force increases linearly in time until a ''rupture force'' is reached signifying a transition between molecular states [Fig. 1(d)]. The transition could physically correspond to, for instance, unfolding of proteins and RNA [2,3] or dissociation of ligand-receptor complexes [4]. Typical outputs from such experiments include distribution of rupture forces $p(F)$, rate of rupture $k(F)$ at a given force F, and mean rupture force $\bar{F}(\dot{F})$ at a given loading rate $\dot{F} \equiv \partial_t F$. Each of these quantities contains information about the intrinsic free energy landscape of the molecule being pulled, namely, the activation barrier height U^*, the barrier distance x^*, and the spontaneous transition rate k_0.

An outstanding theoretical issue concerns the reliable extraction of the above intrinsic kinetics and energetics of molecules from single-molecule pulling experiments. Though recent analytic models [5,6] employing pulling speed as a control parameter have made tremendous progress in tackling this question, their applicability is typically limited to measurements obtained using ''soft'' pulling devices. In other words, the models cannot quantitatively explain differences in the measured distribution of rupture forces when pulling devices of different stiffnesses are used, e.g., optical traps versus atomic force microscope (AFM) or two AFM cantilevers of different stiffnesses. As pointed out recently [7,8], neglection of such stiffness-related effects can have profound consequences on the deduced energetic and kinetic parameters. This inability to properly treat device stiffness leaves the pulling speed as the sole control parameter for generating force measurements, which further limits reliable extraction of U^*, x^*, and k_0, especially if the range of accessible speeds is narrow. In this Letter, we address these pertinent issues in single-molecule biophysics through a theoretical framework that explicitly accounts for the compliance of the pulling device. Our general approach not only elucidates the impact of device stiffness on the measured rupture-force spectrum but facilitates a considerably more reliable extraction of the relevant thermodynamic and kinetic parameters of molecular transitions from force measurements obtained using devices with a wide range of compliances and pulling speeds.

We begin by treating the force-induced molecular transition as a thermally activated escape of a particle over a

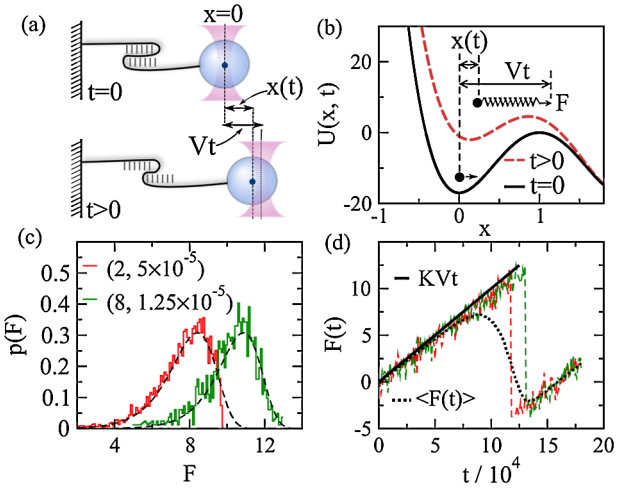

FIG. 1 (color online). (a) Cartoon of a single-molecule pulling experiment. (b) Theoretical analog of (a) showing tilting of the combined free energy landscape with time t due to force F exerted via a spring. (c) Probability distribution of escape forces $p(F)$ for the combination (K, V) [pulling speed: V, pulling spring stiffness: K] so that $KV = 10^{-4}$ from simulation (solid stairs) and the fitted theory Eq. (6) (dashed line). (d) Two sample force traces (dashed lines) and mean force on the particle recorded by the spring $\langle F(t) \rangle$ (dots). In general, $\langle F(t) \rangle < KVt$.

single free energy barrier that is *perturbed* by an external force [Figs. 1(a) and 1(b)]. Accordingly, we can consider the molecule as a particle bound in a free energy landscape $U_0(x)$ and its dynamic microstate is represented by the particle position $x \equiv x(t)$, where the mean start position is $\langle x(0)\rangle = 0$. An external force is impressed via a harmonic spring of stiffness K, which approximates the pulling device. The spring is pulled with speed V such that at time t, the combined free energy surface of the particle and pulling spring can be expressed by

$$U(x, t) = U_0(x) + \frac{1}{2}K(Vt - x)^2. \tag{1}$$

The external force thus "tilts" the energy landscape, diminishing both the barrier height as well as the barrier distance with time [Fig. 1(b)].

An important distinction from previous models is that we do not invoke the soft-spring approximation which would have defined the system free energy as $U(x, t) \approx U_0(x) - KVtx$ and the corresponding perturbing force measured by the spring as $\langle F(t)\rangle = KVt$ where $\langle\cdots\rangle$ denotes an average over many experiments. However, in general, for an arbitrary spring stiffness, one finds that before rupture occurs

$$\langle F(t)\rangle = KVt/\chi \equiv F(t) \tag{2}$$

where $\chi > 1$ is a constant. The origin of χ can be explained by approximating $U_0(x) \approx K_m x^2/2$, where K_m is the curvature of the energy landscape at its minimum. Assuming that the particle relaxes much faster than the time scale of pulling (quasistatic pulling) and that it possesses negligible inertia due to overdamping implies that the mean force acting on it before escape from the energy well is $\langle -\partial_x U(x, t)\rangle \approx 0$. Solving for $\langle x(t)\rangle$ gives $\langle F(t)\rangle = K[Vt - \langle x(t)\rangle] = \frac{KVt}{1+K/K_m}$. The quantity $\chi = 1 + K/K_m$ thus characterizes departure from the soft-spring approximation and is a crucial factor modulating the rupture process as shown later (also see [9]).

Next, we derive expressions for the experimentally accessible quantities: $k(F)$, $p(F)$, and $\bar{F}(\dot{F})$. Using a cubic polynomial $U_0(x) = F_c(x - x^*/2) - F_d(x - x^*/2)^3$ where $F_c \equiv 3U^*/2x^*$ is a critical force and $F_d \equiv 2U^*/x^{*3}$ [5,10,11] with Eq. (1) to evaluate the instantaneous Kramers' escape rate [14,15] and switching the variable from t to F via Eq. (2) yields

$$k(F; \chi) = k_0\left(\chi^2 - \frac{F\chi}{F_c}\right)^{1/2} e^{\beta U^*\{1-[\chi^2-(F\chi/F_c)]^{3/2}\}}. \tag{3}$$

Here, $\chi \equiv \chi(K) = 1 + Kx^{*2}/6U^*$ and k_0 is the rate constant determined at zero force and corresponds to the unperturbed $U_0(x)$.

The above relation implies the rupture rate can be controlled independently via F and χ (i.e., K) (also see [7]). As the exponential term dominates over the prefactor, even small variations in χ resulting from changes in device stiffness are expected to strongly modulate $k(F)$. Further, it hints that the problem of reliably extracting k_0, F_c, and U^* from a master plot [5] with a narrow range of permissible pulling speeds might be overcome by utilizing devices with different stiffnesses.

The probability distribution of rupture times can be expressed as $p(t) = -\frac{ds(t)}{dt} = k(t)s(t)$. Here, $s(t)$ is the survival probability of the particle in its native state at time t. The first equality is a continuity relation while the second [16,17] appears from an asymptotic solution ($\beta U^* \gg 1$) of the Smoluchowski equation assuming negligible barrier recrossing. In constant speed experiments, the above equalities may be rewritten by changing t to F via Eq. (2)

$$p(F) = -\frac{ds(F)}{dF} = \frac{k(F)s(F)}{\dot{F}}. \tag{4}$$

Integrating the second equality in Eq. (4), $\dot{F}\int_1^s ds/s = -\int_0^F k(F)dF$ after substituting Eq. (3) gives

$$F(s) = F_c\chi\left[1 - \left\{1 - \frac{1}{\beta U^*}\ln\left(1 - \frac{\ln s}{\chi^3 qX}\right)\right\}^{2/3}\right] \tag{5a}$$

$$q \equiv \exp[\beta U^*\{1 - \chi^3\}] \approx \exp(-0.5\beta K x^{*2}) \tag{5b}$$

$$X \equiv \frac{k_0}{\beta\chi\dot{F}x^*} = \frac{k_0}{\beta}\frac{1}{KVx^*}. \tag{5c}$$

The approximation in Eq. (5b) is good if $Kx^{*2}/6U^* \ll 1$. Physically X represents the ratio of the intrinsic rate of thermal energy transfer across the barrier k_0/β and the rate at which energy is externally supplied to the molecule KVx^*.

The escape force distribution $p(F)$ can be evaluated by inverting Eq. (5a) to $s(F)$ and substituting in Eq. (4)

$$p(F) = \frac{k(F)e^{qX}}{\dot{F}}\exp\left[-\frac{k(F)}{\beta\dot{F}\chi x^*}\left(\chi^2 - \frac{\chi F}{F_c}\right)^{-(1/2)}\right]. \tag{6}$$

The above expression clearly reflects the importance of two control parameters, K and V, which is also exemplified from the distribution of rupture forces $p(F)$ in Fig. 1(c). The $p(F)$ for these two cases with constant "KV" but distinct K and V will be indistinguishable to the soft-spring based models which enforce $\dot{F} \equiv KV$ as the only control parameter, whereas Eq. (6) (dashed lines) can effectively model the difference.

As collating $p(F)$ requires hundreds of experiments, reporting its mean and standard deviation against $\dot{F}$ from a small number of experiments is more practical. Using the procedure described in Ref. [6], one can derive expressions for $\bar{F} = \int_0^1 F(s)ds$ and σ_F:

$$\bar{F} \cong F_c\chi\left[1 - \left\{1 - \frac{e^{qX}E_1(qX)}{\beta U^*\chi^3}\right\}^{2/3}\right] \tag{7a}$$

$$\sigma_F \equiv \sqrt{\overline{F^2} - \bar{F}^2} \cong \frac{\pi}{\sqrt{6}}\frac{[1 - \frac{e^{qX}E_1(qX)}{\beta U^*\chi^3}]^{-1/3}}{\beta x^*\chi^2(1 + qX)}. \tag{7b}$$

Here, $E_1(u) = \int_u^\infty \frac{e^{-z}}{z}dz$ is the exponential integral [18] which can be approximated as $e^u E_1(u) \approx \ln(1 + e^{-\gamma}/u)$

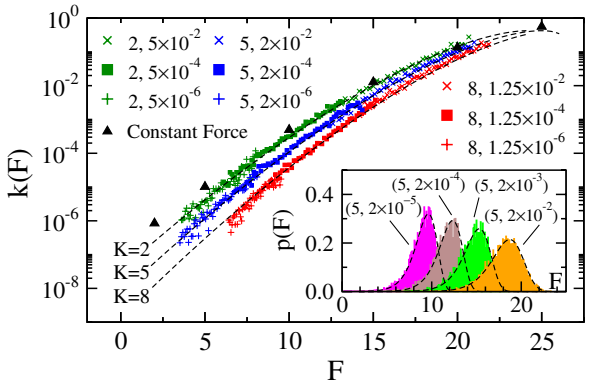

FIG. 2 (color online). Escape rate $k(F)$ as a function of applied force F plotted for different values (K, V) of pulling spring stiffness K and speeds V obtained from simulation (symbols) [5,25]. $k(F)$ obtained from constant-F simulation without using pulling spring is shown by solid triangle symbols. The dashed lines corresponds to Eq. (3). Inset: Probability distribution of escape forces $p(F)$ from simulation (bars), and the dashed lines are fits using Eq. (6).

where $\gamma = 0.577\ldots$ is the Euler constant. Note that when $\chi = 1$ ($q = 1$), Eq. (7) becomes identical to the prediction from soft-spring theory [6].

Equations (3), (6), and (7) provide the necessary expressions that capture the dependence of U^*, x^*, and k_0 on single-molecule force and rate measurements, which can be used to extract these quantities from constant-F and constant-V experiments. To demonstrate the applicability of these expressions, we have performed Brownian dynamics simulations [19] of a particle in an energy well, $U_0(x) = -34x^2 + 17x^4$ [Fig. 1(b)], at $k_BT = 1$ in the constant-V and constant-F setup [20]. In constant-V simulations, the particle is pulled by stiff harmonic springs with $K = 2$, 5, 8 ($\beta K x^{*2}/2 = 1$, 2.5, 4, respectively) whereas for the constant-F simulations, with other conditions remaining unchanged, a fixed force F is applied to the Brownian particle *without* using any pulling spring. Note, however, for practical purposes, very stiff springs can cause barrier recrossings [21], especially at small pulling speeds. This effect occurred negligibly in our simulations.

Figure 2 (solid triangles) shows $k(F)$ from the constant-F simulations and its reduction for the constant-V simulations as the stiffness of pulling spring is raised for all applied forces recorded by the spring, with the strongest reduction observed at low forces. The change in $p(F)$ at constant stiffness as a function of the pulling speed is displayed in Fig. 2 inset (bars). The corresponding spectrum $\bar{F}(\dot{F})$ plotted in Fig. 3 (symbols) also reveals an amplification of rupture force with increasing spring stiffness for all loading rates (cf. [7]). Importantly, we establish good agreement of our expressions, Eqs. (3), (6), and (7) (dashed lines), with their respective simulated results in Fig. 2, Fig. 2 inset, and Fig. 3 using the parameters $U^* = 17$, $x^* = 1$, and $k_0 = 9 \times 10^{-8}$ that correspond to the quartic potential used in our simulations. We also obtain excellent agreement by least-square fitting of data in Fig. 2 with Eq. (3), which yields $U^* = 16.95 \pm 0.32$, $x^* = 1.02 \pm 0.01$, and $k_0 = (8.99 \pm 0.48) \times 10^{-8}$. Note that the theoretical Kramers escape rate for this potential is $k_0 = 3\beta D U^* \exp(-\beta U^*)/\pi x^{*2} = 8.4 \times 10^{-8}$. The excellent agreement between our model, derived using a linear-cubic potential, and simulations, conducted with a quartic potential, emphasizes the generality of the linear-cubic potential in deriving meaningful analytic expressions for the rupture force and rates.

We next enumerate the incongruity in the above estimates if the simulation data with stiff springs are fitted using the soft-spring model: $k(F) = k_0(1 - \frac{F}{F_c})^{1/2} \times \exp[\beta U^*\{1 - (1 - \frac{F}{F_c})^{3/2}\}]$ from Eq. (3) with $\chi = 1$ [5]. We establish good fits (not shown) and extract for $K = 2, 5$ the estimates $U^* = 17.88 \pm 0.24$, $x^* = 1.08 \pm 0.02$, $k_0 = (2.71 \pm 0.28) \times 10^{-8}$, and $U^* = 19.39 \pm 0.24$, $x^* = 1.13 \pm 0.01$, $k_0 = (6.58 \pm 0.05) \times 10^{-9}$, respectively. Thus, compared to the actual energy landscape parameters, the estimates of k_0 can be smaller by as much as an order of magnitude, while U^* and x^* are off by 14% and 11%, respectively (for $K = 5$). Oddly, the above errors arise despite both K values satisfying the soft-spring criteria [5], i.e., $Kx^{*2}/6U^* = 0.02$ and 0.05 ($\ll 1$).

To explain this apparent discrepancy, we consider Eq. (3) in the limit of small forces $F \ll F_c$ and soft springs $Kx^{*2}/6U^* \ll 1$: $k(F) \approx k_0 e^{-\beta K x^{*2}/2} e^{\beta F x^*}$. Clearly, $k(F)$ does not reduce to Bell's expression $k(F) \approx k_0 e^{\beta F x^*}$ [22]. Thus, the requirement for soft-spring approximation is not sufficiently met by the condition $Kx^{*2}/6U^* \ll 1$. In fact, only by choosing $\beta K x^{*2}/2 \ll 1$ can the device stiffness truly be neglected. This then defines the "correct" soft-spring limit. Indeed, the stiff springs ($K = 2, 5$) used in our simulations do *not* satisfy the new soft-spring criterion, i.e., $\beta K x^{*2}/2 = 1$ and 2.5. Further, with $k_0 \propto e^{-\beta U^*}$, one finds $k(F) \propto e^{-\beta(U^* + K x^{*2}/2)}$, which explains why stiff springs enhance barrier heights and lead to slower rupture rates, as captured by both our model and simulations, as well as experiments of others [7,8].

Interestingly, the new soft-spring criterion $K \ll 2/\beta x^{*2}$ is determined by the thermal energy and the barrier distance and *not* by the barrier height. Using a 10% tolerance for error, we obtain a more well-defined criterion $K \lesssim 0.1 \times 2/\beta x^{*2}$. Consider now the rupture of noncovalent bonds (e.g., hydrogen bond) ($x^* \sim 0.2$ nm) and an RNA molecule ($x^* \sim 10$ nm) [3] at room temperature ($1/\beta = 4.1$ pN-nm). Our new criterion states that the soft-spring model [5,6] will be valid if $K \lesssim 5$ pN/nm and 0.002 pN/nm for the noncovalent bond and RNA, respectively. Comparing against typical K values (in pN/nm) of magnetic tweezers (10^{-3}–10^{-6}), optical traps (0.005–1), AFM (10–10^5), and steered molecular dynamics simulation (SMDS) (10^3–10^4) [1], it is clear that force measurements of noncovalent bonds using AFM and SMDS and those of RNA using optical traps, AFM, and SMDS cannot be modeled accurately using the soft-spring model, as the

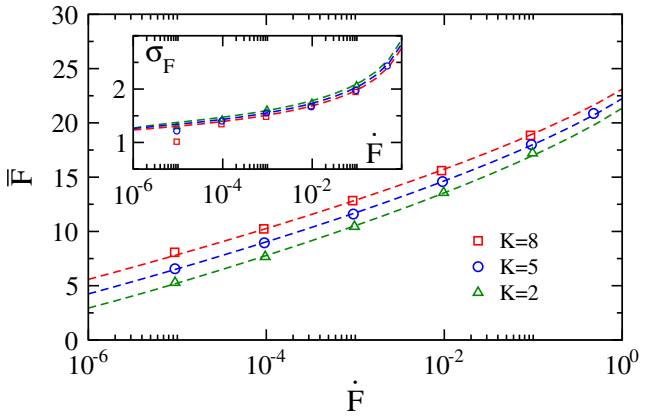

FIG. 3 (color online). Mean escape force $\bar{F}$ from simulation (symbols) plotted against loading rates $\dot{F}$ for three pulling spring stiffness K. Fits from Eq. (7a) are displayed as dashed lines. Inset: The standard deviation σ_F of the escape forces (symbols) and fits of Eq. (7b) are also displayed (dashed lines).

device stiffness will nontrivially magnify observed rupture forces or reduce the rupture rates [17,23,24]. In such cases, the model presented here, which accounts for stiffness effects, will allow correct prediction of the intrinsic kinetic and energetic parameters.

The model developed here has two additional implications. First, rupture-force spectra $\bar{F}(\dot{F})$ retrieved from different techniques are often combined to realize a spectrum over a large range in loading rates to draw the parameters of interest. We emphasize that one has to first ascertain if such a procedure is permissible based on either $K \ll 2/\beta x^{*2}$ or a constant K for all the techniques used. Second, the parameter estimates are prone to errors due to the nonlinearity of the fitting functions and necessitate exploration of a large range of pulling speeds to improve the reliability, which is not always feasible. Our model provides a basis for the utilization of both the pulling speeds and the device itself whose compliance or stiffness can be varied within a reasonable range to improve the free energy parameter estimates by simultaneously fitting the extended space of observables. In conclusion, the analytic model developed here allows for biomolecular pathways and their underlying free energy landscape parameters to be more reliably extracted from single-molecule pulling experiments.

We thank Olga Dudko and Martin Kenward for discussions and comments.

*Corresponding author: garya@ucsd.edu

[1] K. C. Neumann and A. Nagy, Nat. Methods **5**, 491 (2008).
[2] M. Rief, M. Gautel, F. Oesterhelt, J. M. Fernandez, and H. E. Gaub, Science **276**, 1109 (1997).
[3] J. Liphardt, B. Onoa, S. B. Smith, I. Tinoco, and C. Bustamante, Science **292**, 733 (2001).
[4] R. Merkel, P. Nassoy, A. Leung, K. Ritchie, and E. Evans, Nature (London) **397**, 50 (1999).
[5] O. K. Dudko, G. Hummer, and A. Szabo, Phys. Rev. Lett. **96**, 108101 (2006).
[6] R. W. Friddle, Phys. Rev. Lett. **100**, 138302 (2008).
[7] E. B. Walton, S. Lee, and K. J. V. Vliet, Biophys. J. **94**, 2621 (2008).
[8] J. D. Wen, M. Manosas, P. T. X. Li, S. B. Smith, C. Bustamante, and F. Ritort, Biophys. J. **92**, 2996 (2007).
[9] M. Evstigneev and P. Reimann, Phys. Rev. B **73**, 113401 (2006).
[10] A. Garg, Phys. Rev. B **51**, 15592 (1995).
[11] Any smooth function possessing a well-defined minima and maxima can be approximated using a linear-cubic polynomial through a third-order Taylor's expansion about the inflection point [5]. It has also been shown that the linear-cubic potential provides a reasonably good description for single-barrier rupture processes, and that higher-order shape parameters only introduce marginal changes [10,12,13].
[12] M. Evstigneev, Phys. Rev. E **78**, 011118 (2008).
[13] J. Husson and F. Pincet, Phys. Rev. E **77**, 026108 (2008).
[14] H. A. Kramers, Physica (Utrecht) **7**, 284 (1940).
[15] H. Risken, *The Fokker-Planck Equation: Methods of Solutions and Applications* (Springer, Berlin, 1996), 2nd ed., see section 5.10.1; $k(t) = (\beta D/2\pi) \times \sqrt{U''(x^-,t)|U''(x^+,t)|}e^{-\beta\{U(x^+,t)-U(x^-,t)\}}$ where D is the diffusivity and $x = x^-, x^+$ are the positions of the minimum and maximum of the energy landscape.
[16] S. Walcott, J. Chem. Phys. **128**, 215101 (2008).
[17] L. B. Freund, Proc. Natl. Acad. Sci. U.S.A. **106**, 8818 (2009).
[18] M. Abramowitz and I. Stegun, *Handbook of Mathematical Functions* (Dover, New York, 1972).
[19] M. P. Allen and D. J. Tildesley, *Computer Simulation of Liquids* (Clarendon, Oxford, 2004).
[20] Simulations used mass, length, and energy in reduced units with $k_B = 1$, particle mass $m = 1$, friction coefficient $\xi = 8$ ($D = 1/8$), and time step 0.01. The free end of the spring is also moved along the reaction coordinate every time step in the constant-V setup. Spring stiffnesses K satisfies the criterion of overdamped motion $2m/\xi < \sqrt{m/K}$.
[21] Z. Tshiprut, J. Klafter, and M. Urbakh, Biophys. J. **95**, L42 (2008).
[22] G. I. Bell, Science **200**, 618 (1978).
[23] O. K. Dudko, A. E. Filippov, J. Klafter, and M. Urbakh, Proc. Natl. Acad. Sci. U.S.A. **100**, 11378 (2003).
[24] B. Heymann and H. Grubmüller, Phys. Rev. Lett. **84**, 6126 (2000).
[25] Integration of the first equality in Eq. (4) yields $s(F) = \int_F^\infty p(F)dF$ and further from Eq. (4), $p(F)$ can be translated to escape rates: $k(F) = \dot{F}p(F)/\int_F^\infty p(F)dF$.